

Effect of Deposition Rate on Structure and Surface Morphology of Thin Evaporated Al Films on Dielectrics and Semiconductors

Kirill BORDO, Horst-Günter RUBAHN*

NanoSYD, Mads Clausen Institute, University of Southern Denmark, Alsion 2, DK-6400 Sønderborg, Denmark

crossref <http://dx.doi.org/10.5755/j01.ms.18.4.3088>

Received 01 August 2011; accepted 14 September 2011

Aluminum (Al) films with thickness of 100 nm were grown on unheated glass, silicon and mica substrates by electron beam evaporation. The deposition rates were adjusted in the range between 0.1 nm/s and 2 nm/s, the pressure in the vacuum chamber during deposition was lower than $1 \cdot 10^{-3}$ Pa. The structure and surface morphology of the as-deposited Al films were studied using scanning electron microscopy (SEM) and atomic force microscopy (AFM). SEM imaging of the films showed that the mean grain size of thin Al films on all of the substrates increased from 20 nm–30 nm to 50 nm–70 nm with increase of the deposition rate. Quantitative AFM characterization showed that for all substrates the root mean square surface roughness increases monotonically with increasing the deposition rate from 0.1 nm/s to 2 nm/s. The observed effects of the deposition rate on the grain size and surface roughness are explained by the fundamental characteristics of the island growth mode, the influence of the background gases and the surface morphology of the bare substrates.

Keywords: aluminum thin films, e-beam evaporation, deposition rate, grain size, surface roughness.

1. INTRODUCTION

Aluminum in the form of thin evaporated films has numerous applications in different branches of modern technology. It is known to be one of the most important materials for microelectronics, where it is used for the fabrication of interconnects and Ohmic contacts [1]. Because of its high reflectance and good adherence to glass, evaporated aluminum is the most frequently used coating for optical mirrors [2, 3]. Other applications of thin evaporated aluminum films include near-field fiber-optic probes [4], thin film transistors [5], flat panel displays [6] and solar cells [7].

For all these reasons, the properties of thin Al films produced by e-beam or thermal evaporation have been extensively studied by a number of research groups [2–4, 8–19]. It is known that structural and therefore also electrical and optical properties of thin metallic films are affected by a few factors, namely by the type of the substrate [20–23], the thickness of the film [12, 13, 15, 17], the deposition rate [13, 14, 16, 21, 22, 24], the temperature of the substrate [8, 11, 16, 22], the annealing conditions [9, 17] and the background gas composition [4, 14].

The deposition rate is one of the most important parameters influencing the structure and surface morphology of the resulting thin films. In principle, this parameter can be readily controlled during the fabrication process. Semaltianos [13] studied thin Al films produced on quartz substrates by evaporation from a boat at rates from 0.1 nm/s to 2 nm/s. It was found that the root mean square (rms) roughness of the 22 nm thick Al films increases from about 3.2 nm to 5 nm with an increase of the rate from 0.2 nm/s to 1.5 nm/s. Qui et al. [14] investigated the influence of the deposition rate on the structure, composition and resistivity of thin Al films produced by e-beam evaporation on glass at two rates: 0.17 nm/s and 0.55 nm/s.

The film prepared at higher deposition rate had larger grain size but lower roughness than the one made at lower rate. Higo et al. [16] did not observe any change in the surface roughness of 200 nm thick evaporated Al films on mica as the deposition rate increased from 0.5 nm/s to 2 nm/s. Data on the rate-dependent properties of thin evaporated Al films on silicon, as well as data for a wide range of deposition rates for glass and mica, are lacking so far in the literature. In the present paper, we investigate the structure and surface morphology of thin Al films produced by e-beam evaporation on three different substrates (silicon, glass and mica), as a function of deposition rate within a wide range of rates (from 0.1 nm/s to 2 nm/s). The as-prepared films are studied by means of scanning electron microscopy (SEM) and atomic force microscopy (AFM); the results are cross-compared and briefly discussed.

2. EXPERIMENTAL

A conventional electron beam evaporation system (Edwards Auto 500) equipped with an oil-free turbomolecular pumping system was used in the present work. The film thickness and deposition rate were controlled by a quartz microbalance. Aluminum films with a thickness of about 100 nm were deposited on unheated silicon, glass or mica substrates using a high-purity (99.99 %) Al target placed into an intermetallic (BN-TiB₂) crucible liner. The films were produced at 5 different evaporation rates: 0.10 ± 0.02 , 0.20 ± 0.02 , 0.5 ± 0.1 , 1.0 ± 0.1 and 2.0 ± 0.2 nm/s. The required evaporation rate was achieved by adjusting the e-beam current. The pressure in the chamber during deposition was better than $1 \cdot 10^{-3}$ Pa. The acceleration voltage of the electron gun was fixed at 4.76 kV and the e-beam current was kept in the range between 20 mA and 80 mA, depending on the required evaporation rate and the load of the crucible.

The silicon (Si (100), *p*-type, resistivity (1–100) Ohm·cm⁻¹) and glass (BK7) substrates were pre-cleaned by ultrasonication in acetone and ethanol (5 min. in each

*Corresponding author. Tel.: +45-6550-1657; fax.: +45-6550-1657.
E-mail address: rubahn@mci.sdu.dk (H.-B. Rubahn)

solvent) followed by oxygen plasma etching (5 min. at 300 W, Branson IPC 3000 barrel plasma system). The muscovite mica substrates (grade V-3, Plano GmbH) were cleaved in air and transferred thereafter immediately into the deposition chamber.

The SEM imaging of the evaporated thin Al films was performed in a commercial instrument (Hitachi S-4800) with an acceleration voltage of 2 kV–3 kV. The ranges of grain size of the films were obtained by picking randomly 20 grains on each SEM image and estimating their equivalent diameters.

The AFM characterization was performed using a Dimension 3100 AFM (Digital Instruments, Veeco, CA) operated in tapping mode. The topographic and phase images were recorded simultaneously using a standard silicon tip with radius 10 nm. The spring constant of the cantilever was between 20 N/m and 100 N/m. Root mean square (rms) surface roughness values were determined for each sample on an area of $(30 \times 30) \mu\text{m}^2$. Rms surface roughness values were calculated using free SPM analysis software (Gwyddion [25]).

3. RESULTS

3.1. SEM

SEM imaging of thin evaporated Al films allowed us to observe the microstructure of the films as a function of deposition rate and to estimate the grain size.

Fig. 1 shows representative SEM images of thin Al films evaporated onto silicon substrates at different deposition rates from 0.1 nm/s to 2 nm/s.

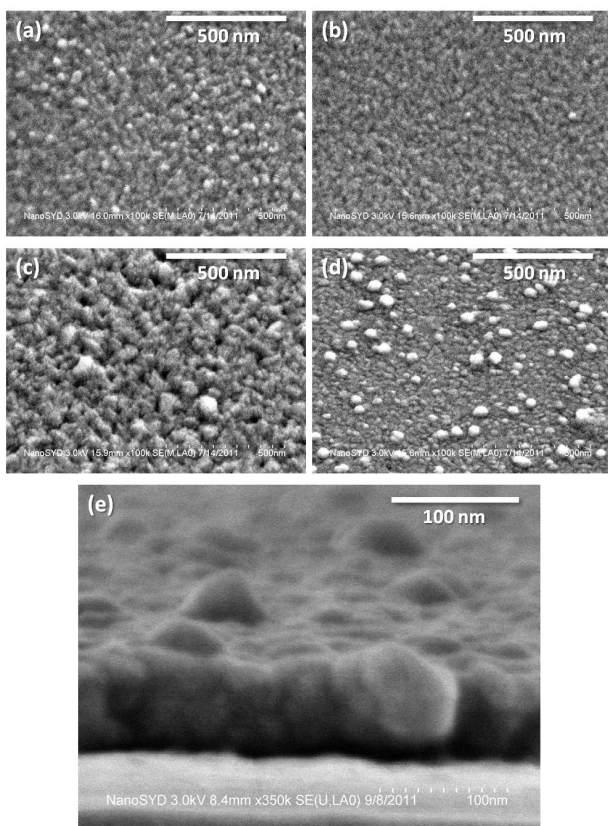


Fig. 1. SEM images of thin Al films produced on silicon substrates at different deposition rates: 0.1 nm/s (a), 0.5 nm/s (b), 1 nm/s (c) and 2 nm/s (d, e); (e) is the cross-sectional view of the film shown on (d)

In order to achieve a better contrast for the film structure, the top view images (Fig. 1, a–d) were obtained with the SEM stage being tilted by 45° with respect to the horizontal position. For all of the films, a grainy surface structure with well-defined individual grains and voids between them is observed. The films produced at the lower deposition rate (0.1 nm/s) exhibit a rather smooth grainy surface. The grains have spherical or oval shape and are almost uniform in size. The films produced at higher rates (1 nm/s–2 nm/s) exhibit single outgrowths (hillocks) protruding out from the film surface. The density of the hillocks increases with an increase in the deposition rate.

The ranges of grain size (nm) of the deposited thin Al films, estimated from the SEM images, are presented in Table 1.

Table 1. Ranges of grain size (nm) of thin Al films evaporated on glass, silicon and mica substrates at different deposition rates, as estimated from SEM images

Deposition rate, nm/s	Substrate		
	Glass	Silicon	Mica
0.1	20–40	15–30	15–30
0.2	20–40	15–40	15–30
0.5	20–50	20–40	20–40
1.0	30–70	20–70	30–70
2.0	40–100	30–80	40–100

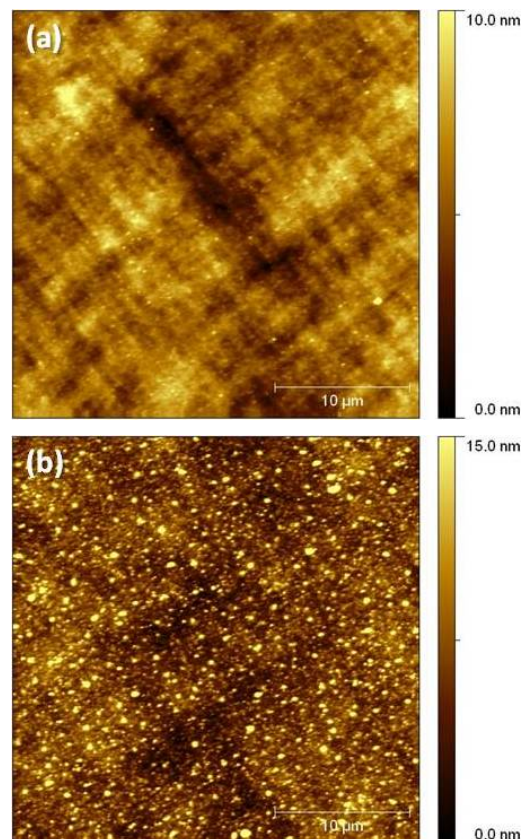


Fig. 2. AFM images $((30 \times 30) \mu\text{m}^2)$ of 100 nm thick Al films evaporated on silicon substrates at 0.5 nm/s (a) and 2 nm/s (b)

It can be seen that the average grain size increases monotonically with increase in deposition rate. At low deposition rates (0.1 nm/s–0.2 nm/s) the films consist of small grains with almost uniform size (in the range between 15 nm and 40 nm). At higher rates (1 nm/s–2 nm/s) large

hillocks having size of 50 nm–100 nm appear on the film surface. At the same time, there are still a lot of smaller (20 nm–50 nm) grains in the areas between the hillocks. Thus, the grain size distributions of the as-deposited Al films become wider with increase in deposition rate.

3.2. AFM

The surface morphology of the thin Al films on different substrates was investigated by tapping mode AFM as a function of deposition rate. Root mean square surface roughness values were determined on an area of $(30 \times 30) \mu\text{m}^2$. For each of the samples, including bare glass, silicon and mica substrates, 5 scans of the same area at the same scanning parameters were performed.

Fig. 2 shows typical AFM scans of 100 nm thick Al films evaporated onto silicon substrates at two deposition rates: 0.5 nm/s and 2 nm/s. It can be seen that at the lower deposition rate of 0.5 nm/s (Fig. 2, a) the Al film is rather smooth but exhibits a grainy morphology. For the higher deposition rate of 2 nm/s (Fig. 2, b) the same kind of surface morphology is observed; however, the film consists of bigger grains and there are more big hillocks on the surface.

In Table 2, rms surface roughness for thin Al films, produced on different substrates at different deposition rates, are summarized.

Table 2. Rms surface roughness (nm) of thin Al films evaporated on glass, silicon and mica substrates, as a function of deposition rate. The mean values are obtained from 5 scans of $(30 \times 30) \mu\text{m}^2$ size on each sample

Deposition rate, nm/s	Substrate		
	Glass	Silicon	Mica
0 (bare substrate)	1.06 ± 0.22	1.24 ± 0.20	0.25 ± 0.05
0.1	1.12 ± 0.09	1.25 ± 0.10	0.67 ± 0.11
0.2	1.23 ± 0.13	1.30 ± 0.18	1.10 ± 0.17
0.5	1.6 ± 0.5	1.51 ± 0.25	1.46 ± 0.15
1	2.0 ± 0.6	1.73 ± 0.19	1.8 ± 0.4
2	4.1 ± 0.7	3.6 ± 0.7	3.8 ± 0.6

As can be seen from the data presented, the rms roughness of as-produced Al films increases significantly as the deposition rate is increased from 0.1 nm/s to 2 nm/s. For low rates (0.1 nm/s–0.2 nm/s) the roughness of the films correlates well with the roughness of the bare substrates. In particular, the films deposited on mica are much smoother than the ones evaporated on glass and silicon.

4. DISCUSSION

In the present work, the microstructure of thin evaporated Al films was observed and evaluated by SEM and AFM. The former technique provides general information about the surface structure (shape and size of grains), while the latter technique allows quantitative characterization of the surface morphology, including e. g. the determination of surface roughness.

As can be seen from SEM images (Fig. 1), all the Al films exhibit a grainy structure with well defined columnar grains separated by voids. This kind of structure was observed for many evaporated and sputtered films [26–30]. In order to describe it, the so-called structure zone model

was proposed [26, 27]. According to this model, the film surface structure is dominated by the substrate temperature (T). There are 3 main structure zones with boundary temperatures $T_1 = 0.3T_m$ and $T_2 = 0.5T_m$, where T_m (K) is the melting point of the film material. At relatively low temperatures ($T < T_1$, zone 1), the surface diffusion of adatoms is too weak to ensure the filling of the shadowed surface regions (self-shadowing effect). That leads to the formation of the characteristic well-defined columnar structure. The films deposited at higher temperatures ($T_1 < T < T_2$, zone 2) exhibit much larger columns with domed tops. The surface diffusion of adatoms becomes sufficient which leads to surface recrystallization under these conditions. The films deposited at $T > T_2$ (zone 3) consist of big grains with flat and faceted faces [27].

In the present work, the Al films were deposited at room temperature (20°C , $T/T_m = 0.31$ for Al) which corresponds to the boundary between zone 1 and zone 2. Even if a slight heating of the substrates by radiation from the evaporation source takes place, that should not lead to any significant changes in the films structure, according to the zone model. Therefore, the observed difference in the structure and morphology of the films is most probably caused by deposition rate effects.

From the SEM images, the average grain size of the Al films prepared at different evaporation rates was estimated. The results are presented in Fig. 3. It can be seen that for all substrates the average grain size increases monotonically with increase in deposition rate. For films deposited onto different substrates at the same rate, the grain size ranges are approximately the same (see also Table 1).

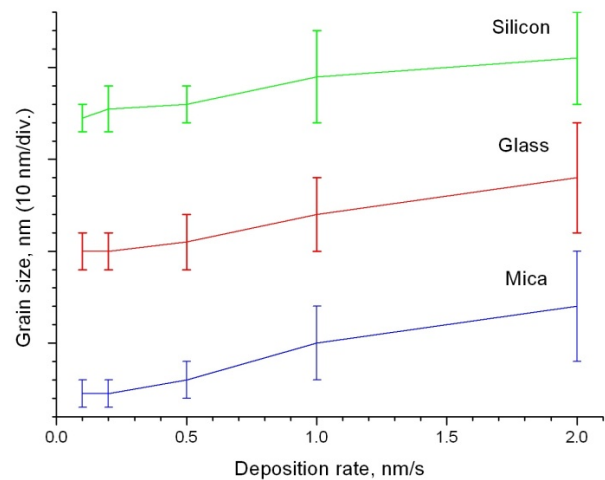


Fig. 3. Range of grain size (estimated from SEM images) of thin Al films evaporated on glass, silicon and mica substrates as a function of deposition rate

The observed dependence of grain size on deposition rate is consistent with the results obtained by Semaltianos [13] for thin evaporated Al films on quartz and also with the results reported by Cai et al. [24] for thin evaporated Ti films on glass. This trend can be explained by considering the processes of surface diffusion of adatoms and nucleation and coalescence of metal clusters during deposition [30]. The Al atoms arriving onto the substrate surface can diffuse along the surface and form clusters which can in turn contribute to the formation of crystallites (grains). At low evaporation rates and low substrate

temperatures, the surface diffusion of the Al atoms and formation of Al clusters is not prominent. Therefore the density of clusters (nuclei) which can potentially coalesce to form grains is small, resulting in a small grain size. At higher deposition rates, the number of Al atoms arriving onto the surface per unit time is higher. Consequently the number of nuclei formed on the surface is bigger which leads to the formation of bigger grains.

In addition to the mechanism described above, the residual gases such as oxygen are considered to affect the growth of the individual grains [14, 30]. The adsorbed oxygen and/or oxide precipitates, which accumulate on the surface of growing crystallites, can suppress the crystallite growth. The ratio of the number of residual gas atoms impinging on the substrate or the film surface to the number of film atoms arriving to the substrate or the film surface per time and area (in other words, the concentration of residual gas atoms in the film) is inversely proportional to the deposition rate [14]. Thus it can be assumed that at given temperature, pressure and residual gas composition, the concentration of residual gas atoms in the film decreases by a factor of 20 with increase in the deposition rate from 0.1 nm/s to 2 nm/s. Therefore increasing the deposition rate within the stated range should significantly weaken the influence of the residual gas atoms on the grain growth and allow the formation of bigger grains.

Surface roughness of metal thin films and coatings is known to influence their properties (such as wear and corrosion resistance, reflectivity, etc.) which are critical for practical applications. In the present work, the surface roughness of the thin evaporated Al films was determined from AFM data. For each of the samples 5 scans of the same area ($(30 \times 30) \mu\text{m}^2$) at the same scanning parameters were obtained. The dependence of the rms surface roughness on the deposition rate is shown in Fig. 4 (for uncertainties, refer to Table 2).

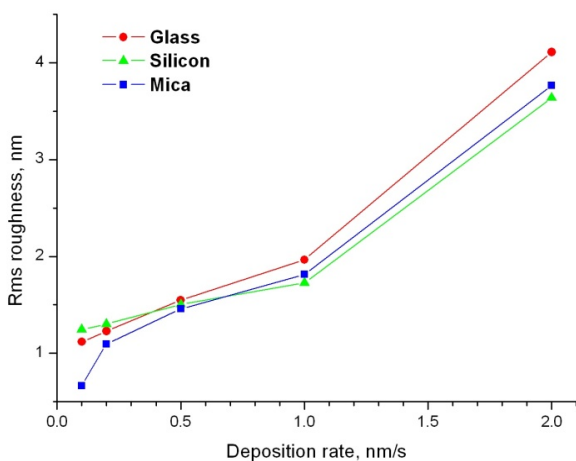


Fig. 4. Rms surface roughness (obtained from 5 scans of $30 \times 30 \mu\text{m}^2$ size on each sample) of thin Al films evaporated on glass, silicon and mica substrates as a function of deposition rate

It can be seen that the rms roughness of the Al films on all substrates increases monotonically with increase of the deposition rate. These results agree with the data reported by Semaltianos [13] but they are not consistent with the data presented by Qui et al. [14] who observed a decrease in the roughness of Al films on glass from 2.5 nm to

1.5 nm with an increase of deposition rate from 0.17 nm/s to 0.55 nm/s. However in the latter study only single values of roughness were presented which were determined from very small areas ($(0.5 \times 0.5) \mu\text{m}^2$). In such a case the value of surface roughness on a bigger scale (tens of μm), arising from the large grains and hillocks formed at high deposition rates, might be underestimated.

It is known that the main factors contributing to the roughening of evaporated metal films are self-shadowing (mentioned above) and statistical roughening. The self-shadowing effect leads to the formation of the characteristic columnar structure of thin films in zone 1, according to the zone model [26, 27]. Statistical roughening is caused by the statistical fluctuation of the vapor flux. This phenomenon also causes the increase in surface roughness with an increase of film thickness [13, 30]. The increase of surface roughness for the Al films under investigation agrees well with the increase in average grain size estimated from the SEM images. At lower deposition rates (0.1 nm/s–1 nm/s) the roughness is determined by the size of the columnar grains and the depths of the voids between them. At the higher rate of 2 nm/s the significant increase in roughness is apparently related to the big number of large hillocks protruding out from the film surface.

It should be noted that at low deposition rates (0.1 nm/s–0.2 nm/s) the roughness of the Al films correlates well with the roughness of the bare substrates. In particular, the films deposited on mica are significantly smoother (rms roughness 0.25 nm–0.67 nm) than the ones evaporated on glass and silicon (rms roughness higher than 1 nm). At higher deposition rates (0.5 nm/s–2 nm/s) the roughness of the films deposited on different substrates has very similar values for each rate. It is known [31] that a thin film can mimic some morphology features from the substrate. Apparently, for 100 nm thick Al films which are evaporated at low rates and consist of fine grains, this effect is rather prominent. At higher rates, the overall coarsening of the surface structure does not allow us to observe any correlation between the roughness values of the Al films and that of the bare substrates.

5. CONCLUSIONS

In the present work, thin Al films with thickness of 100 nm were prepared by e-beam evaporation on three different substrates: glass, silicon and mica. The pressure in the vacuum chamber during deposition was lower than $1 \cdot 10^{-3}$ Pa. The surface structure and morphology were investigated as a function of deposition rate within a wide range of rates: from 0.1 nm/s to 2 nm/s.

SEM imaging of the as-prepared films reveals a grainy structure, with the grain size and overall roughness being strongly dependent on the deposition rate. The films produced at higher rates (1 nm/s–2 nm/s) exhibit outgrowths (hillocks) the density of which increases with increase in deposition rate. The mean grain size increases for Al films on all substrates from 20 nm–30 nm to 50 nm–70 nm with increase of deposition rate.

Quantitative AFM characterization reveals a strong dependence of the surface roughness of the deposited films on the evaporation rate. For all substrates, the root mean

square surface roughness increases monotonically with increasing the deposition rate from 0.1 nm/s to 2 nm/s. For low rates (0.1 nm/s–0.2 nm/s) the roughness of the films correlates well with the roughness of the bare substrates.

Three main factors are believed to be responsible for the observed dependence of the grain size and surface roughness on the deposition rate. They are: (1) the characteristic features of the island growth mode (surface diffusion of adatoms, nucleation and coalescence of Al clusters); (2) influence of the residual gases (in particular oxygen), which can be incorporated into the film during deposition, on the grain growth; (3) the surface morphology of the corresponding bare substrates.

Acknowledgments

We would like to thank Kasper Thilising-Hansen (NanoSYD) for help with the AFM measurements and Jacek Fiutowski (NanoSYD) for help with the preparation of glass and silicon substrates.

REFERENCES

1. **Plummer, J. D., Deal, M. D., Griffin, P. B.** Silicon VLSI Technology: Fundamentals, Practice and Models. Prentice Hall, NJ, 2000: 817 p.
2. **Hass, G., Waylonis, J. E.** Optical Constants and Reflectance and Transmittance of Evaporated Aluminum in the Visible and Ultraviolet *Journal of the Optical Society of America* 51 1961: pp. 719–722.
3. **Guenther, K., Penny, I., Willey, R. R.** Corrosion-resistant Front Surface Aluminum Mirror Coatings *Optical Engineering* 32 1993: pp. 547–552. <http://dx.doi.org/10.1117/12.60845>
4. **Hollars, C. W., Dunn, R. C.** Evaluation of Thermal Evaporation Conditions Used in Coating Aluminum on Near-field Fiber-optic Probes *Review of Scientific Instruments* 69 1998: pp. 1747–1752.
5. **Takatsuji, H., Arai, T.** Pinholes in Al Thin Films: Their Effect on TFT Characteristics and a Taguchi Method Analysis of Their Origins *Vacuum* 59 2000: pp. 606–613.
6. **Voutsas, A. T., Hibino, Y., Pethe, R., Demaray, E.** Structure Engineering for Hillock-free Pure Aluminum Sputter Deposition for Gate and Source Line Fabrication in Active-matrix Liquid Crystal Displays *Journal of Vacuum Science and Technology A* 16 1998: pp. 2668–2667.
7. **Shinohara, H., Morooka, H., Ikeo, I., Takenouchi, A., Nakajima, S., Arai, Y.** Solar Cell and Method for Producing Electrode for Solar Cell. United States Patent US005891264A, 1999.
8. **Starý, V.** Epitaxial Growth of Al Thin Films on Mica and Investigation of Film Structure *Czechoslovak Journal of Physics B* 26 1976: pp. 882–889.
9. **Flinn, P. A., Gardner, D. S., Nix, W. D.** Measurement and Interpretation of Stress in Aluminum-based Metallization as a Function of Thermal History *IEEE Transactions on Electron Devices* V ED-34 No. 3 March 1987.
10. **Ericson, F., Kristensen, N., Schweitz, J.-Å., Smith, U.** A Transmission Electron Microscopy Study of Hillocks in Thin Aluminum Films *Journal of Vacuum Science and Technology B* 9 1991: pp. 58–63.
11. **Higo, M., Lu, X., Mazur, U., Higgs, K. W.** Preparation of Atomically Smooth Aluminium Films: Characterization by Transmission Electron Microscopy and Atomic Force Microscopy *Langmuir* 13 1997: pp. 6176–6182.
12. **Quintana, P., Oliva, A. I., Ceh, O., Corona, J. E.** Thickness Effects on Aluminum Thin Films *Superficies y Vacío* 9 1999: pp. 280–282.
13. **Semaltianos, N. G.** Thermally Evaporated Aluminium Thin Films *Applied Surface Science* 183 2001: pp. 223–229. [http://dx.doi.org/10.1016/S0169-4332\(01\)00565-7](http://dx.doi.org/10.1016/S0169-4332(01)00565-7)
14. **Qui, H., Wang, F., Wu, P., Pan, L., Li, L., Xiong, L., Tian, Y.** Effect of Deposition Rate on Structural and Electrical Properties of Al Films Deposited on Glass by Electron Beam Evaporation *Thin Solid Films* 414 2002: pp. 150–153.
15. **Aguilar, M., Quintana, P., Oliva, A. I.** Thickness-stress Relations in Aluminum Thin Films *Materials and Manufacturing Processes* 17 2002: pp. 57–65.
16. **Higo, M., Fujita, K., Mitsushio, M., Yoshidome, T., Kakoi, T.** Epitaxial Growth and Surface Morphology of Aluminum Films Deposited on Mica Studied by Transmission Electron Microscopy and Atomic Force Microscopy *Thin Solid Films* 516 2007: pp. 17–24.
17. **Hwang, S.-J., Lee, J.-H., Jeong, C.-O., Joo, Y.-C.** Effect of Film Thickness and Annealing Temperature on Hillock Distributions in Pure Al Films *Scripta Materialia* 56 2007: pp. 17–20.
18. **Guisbiers, G., Van Overschelde, O., Wautelet, M., Leclère, Ph., Lazzaroni, R.** Fractal Dimension, Growth Mode and Residual Stress of Metal Thin Films *Journal of Applied Physics D: Applied Physics* 40 2007: pp. 1077–1079.
19. **Hosseinabadi, S., Mortezaali, A., Masoudi, A. A.** Investigating Aluminum Thin Films Properties by Stochastic Analysis *Surface and Interface Analysis* 40 2008: pp. 71–75.
20. **Podbrdský, J., Drahoš, V.** Electron Microscope Study of Aluminium Films Evaporated on Air-cleaved Sodium Chloride *Czechoslovak Journal of Physics B* 19 1969: pp. 217–221.
21. **Semin, D. J., Rowlen, K. L.** Influence of Vapor Deposition Parameters on SERS Active Ag Film Morphology and Optical Properties *Analytical Chemistry* 66 1994: pp. 4324–4331
22. **Higo, M., Fujita, K., Tanaka, Y., Mitsushio, M., Yoshidome, T.** Surface Morphology of Metal Films Deposited on Mica at Various Temperatures Observed by Atomic Force Microscopy *Applied Surface Science* 252 2006: pp. 5083–5099.
23. **Quade, U. J., Pantleon, K.** Orientationally Ordered Ridge Structures of Aluminum Films on Hydrogen Terminated Silicon *Thin Solid Films* 515 2006: pp. 2066–2072.
24. **Cai, K., Müller, M., Bossert, J., Rechtenbach, A., Jandt, K. D.** Surface Structure and Composition of Flat Titanium Films as a Function of Film Thickness and Evaporation Rate *Applied Surface Science* 250 2005: pp. 252–267.
25. Gwyddion – Free SPM Data Analysis Software, <http://gwyddion.net/>
26. **Movchan, B. A., Demchishin, A. V.** Poluchenie pokrytij pri vakuumnoj kondensatsii metallov i splavov *Physics of Metals and Metallography* 28 1969: pp. 83–90.
27. **Thornton, J. A.** High Rate Thick Film Growth *Annual Review of Materials Science* 7 1977: pp. 239–260. <http://dx.doi.org/10.1146/annurev.ms.07.080177.001323>
28. **Thornton, J. A.** The Microstructure of Sputter-deposited Coatings *Journal of Vacuum Science and Technology A* 4 1986: pp. 3059–3065.
29. **Westra, K. L., Thomson, D. J.** The Microstructure of Thin Films Observed Using Atomic Force Microscopy *Thin Solid Films* 257 1995: pp. 15–21.
30. **Smith, D. L.** Thin-film Deposition: Principles and Practice. McGraw-Hill, Inc., New York, 1995: 616 p.
31. **Sellner, S., Gerlach, A., Kowarik, S., Schreiber, F., Dosch, H., Meyer, S., Pflaum, J., Ulbricht, G.** Comparative Study of the Growth of Sputtered Aluminum Oxide Films on Organic and Inorganic Substrates *Thin Solid Films* 516 2008: pp. 6377–6381.